OPENQUATERNARY

Hausmann, N, et al. 2019. Annual Growth Patterns and Interspecimen Variability in Mg/Ca Records of Archaeological Ostrea edulis (European Oyster) from the Late Mesolithic Site of Conors Island. *Open Quaternary*, 5: 9, pp. 1–18. DOI: https://doi.org/10.5334/oq.59

RESEARCH PAPER

Annual Growth Patterns and Interspecimen Variability in Mg/Ca Records of Archaeological *Ostrea edulis* (European Oyster) from the Late Mesolithic Site of Conors Island

Niklas Hausmann*,†, Harry K. Robson† and Chris Hunt‡

Annual growth patterns in marine mollusc shells are valuable indicators of the condition of marine ecology through time. In archaeological contexts, the mollusc's time of death (i.e. the last season of growth) is an indicator of human exploitation patterns throughout the year, enabling the reconstruction of when and how often gathering occurred as well as when sites were occupied. Both pieces of information, growth rate and season of death, are vital for understanding exploitation pressure(s) in the past, and building baselines for modern environmental policies that secure sustainable marine resources. Previously, these parameters have been determined by incremental growth-line or isotopic analyses, which are time consuming and often expensive techniques, thus restricting sample size and the overall robustness of palaeoecological interpretations.

Here, we apply Laser Induced Breakdown Spectroscopy (LIBS) to produce elemental maps (Mg/Ca) with the potential to trace and display growth patterns quickly, and at a reduced cost. We further compare the elemental maps with the results obtained from incremental growth-line analysis to provide a structural context for the geochemical data, and demonstrate the utility of an integrated methodological approach.

Our pilot study was undertaken on 12 European oysters (*Ostrea edulis*, Linnaeus, 1758) from the Late Mesolithic shell midden at Conors Island, Co. Sligo in the Republic of Ireland. Our LIBS analysis enabled us to accurately and quickly determine repeating growth patterns, which were often in agreement with the annual growth increments visible through the microscopic analysis. Based on this comparative dataset, including structural and geochemical patterns, the Late Mesolithic site of Conors Island had been occupied throughout the year. Moreover, our analyses highlight the applicability of LIBS to determine prehistoric seasonality practices as well as biological age and growth at an improved rate and reduced cost than was previously achievable.

Keywords: Mesolithic; *Ostrea edulis*; Laser Induced Breakdown Spectroscopy; Incremental growth line analysis. Seasonality; ecological baseline

1. Introduction

Ostreidae (oysters) are a family for which growth data are frequently needed. Indeed, information on growth rates and population dynamics of *Ostrea edulis* (European oyster, Linnaeus, 1758) are important for the conservation, restoration, and management of modern (Kraeuter et al. 2007; Powell et al. 2008; Harding et al. 2010; Levinton et al. 2013; Baggett et al. 2015), and past populations (Rick and Lockwood 2013; Rick et al. 2016, 2017; Kusnerik et al. 2018).

Ecosystems from a range of periods have been assessed through incremental growth-line analyses, including prehistoric as well as pre-industrial or modern datasets, giving detailed information on marine ecosystems, habitats or the ecological behaviour of early hunter-gatherer-fisher communities (Kirby and Miller 2005; Blitz et al. 2014; Rick et al. 2016, 2017). Whilst studies undertaken on the European oyster have a long research history (Orton 1928; Walne 1958; Grant et al. 1990), the application of incremental growth-line analysis has only been relatively recently employed on archaeological materials (Milner 2001, 2002, 2005; Bailey and Milner 2008; Milner and Laurie 2009; Robson 2015). In this context, incremental growth-line analysis and – now more commonly – oxygen isotope ($\delta^{18}O$) analysis have largely focussed on determining the season and age-of-death of individual specimens, a common method in archaeology to explore prehistoric consumption patterns, site seasonality, including mobility

* Institute of Electronic Structure and Laser, Foundation for Research and Technology, Hellas (IESL-FORTH), Heraklion, Crete, GR

† Department of Archaeology, BioArCh, University of York, York, UK

‡ Natural Sciences and Psychology, Liverpool John Moores University, Liverpool, UK

Corresponding author: Niklas Hausmann (niklas@palaeo.eu)

patterns, and ritual behaviours (Mannino et al. 2003; Blitz et al. 2014; Prendergast and Stevens 2014; Hausmann and Meredith-Williams 2017a; West et al. 2018; see also Twaddle et al. 2016; Burchell et al. 2018).

Incremental growth-line analysis makes use of seasonally or annually predictable changes in the growth structure of shells (i.e. regular periods of growth and cessations in growth that are visible as distinct edges or lines) (Lutz and Rhoads 1977; Lutz and Rhoads 1980; Fan et al. 2011; Zimmt et al. 2019). Depending on the resolution under which incremental growth-lines are examined, their analysis is more or less labour-intensive. For instance, thin sectioning and high-resolution incremental growth-line analysis is very time consuming (Hallmann et al. 2009), and can require specific training to differentiate between annual and disturbance lines (Milner 2001). In contrast, low-resolution incremental growth-line analysis of sectioned but lightly polished oysters are less time consuming (Zimmt et al. 2019), but can experience problems in accuracy, when regular growth segments are intermixed with and indistinguishable from irregular and unpredictable growth structures as is the case in some geographic regions (Andrus 2011; Tynan et al. 2017). One way of contextualising irregular shell growth in oysters are geochemical proxies for seasonally occurring environmental changes (see also Surge et al. 2001; Lulewicz et al. 2018; Zimmt et al. 2019); the most established proxy being $\delta^{18}O$ isotope analysis, which in shell carbonates primarily reflects the $\delta^{18}O$ values of the immediate environment and temperature during the calcification process (Epstein et al. 1953; Grossman and Ku 1986). However, this approach requires a general understanding of the growth structure, a sampling resolution that appropriately covers this structure to provide a seasonal resolution (West et al. 2018), and lastly expensive mass spectrometric analysis.

The above methodological constraints of cost and processing time are detrimental to acquiring large sample sizes while maintaining analytical accuracy, which ultimately has a negative effect on the overall robustness of population-wide studies. For this reason, researchers more often head towards reliable and faster methods for determining the ages and growth rates of molluscs (Durham et al. 2017; Zimmt et al. 2019). For instance, Durham et al. (2017) applied a fast geochemical approach using LA-ICP-MS (Laser-Ablation-Inductively Coupled Plasma-Mass Spectrometry), that exceeded the sampling and analytical speed of $\delta^{18}O$ isotopic or high-quality elemental (Nano-SIMS) methods. Through rapid scanning they showed repeating changes in Mg/Ca ratios connected to annual changes in growth rates of the American oyster (*Crassostrea virginica*, Gmelin, 1791). These patterns were predictably occurring *per annum* and are thus reliable indicators for the specimens' biological age and likely also the season of death.

Building on this, we employed the spectroscopic method of Laser Induced Breakdown Spectroscopy (LIBS), which has recently been used as a fast elemental mapping technique for mollusc shells (Hausmann et al. 2017; Hausmann et al. 2019a), has been shown to reach analytical speeds of over 300,000 measurements per hour (Cáceres et al. 2017), and requires little sample preparation (Cobo et al. 2015; García-Escárzaga et al. 2015; Cobo et al. 2017; Hausmann et al. 2019b). We aim to explore the use of LIBS to create 2-dimensional maps of Mg/Ca ratios, and relate these 2D patterns to the incremental growth structures of the European oyster obtained via microscopic analysis. Specifically, this pilot study involved the analyses of 12 archaeological shells from the shell midden site at Conors Island, Co. Sligo in the Republic of Ireland, which dates to the Late Mesolithic.

By providing a fast and reliable elemental approach to studying growth structures, we provide the foundation to overcome the common problem of small sample sizes, often found in archaeological seasonality and ecological studies.

1.1. An overview of the Irish Mesolithic and shell middens

Ireland has a unique prehistoric record, which is the result of its position on the far northwestern margin of Europe (Waddell 2010). Since Ireland was overridden by highly-erosive glaciers at the Last Glacial Maximum and became an island *ca.* 16,000 cal BP (Edwards and Brooks 2008), Palaeolithic archaeology is scant. A recent AMS radiocarbon (^{14}C) dating programme has, however, demonstrated that Ireland had been colonised, perhaps by boat, around the beginning of the Younger Dryas (Dowd and Carden 2016; Little et al. 2017). The Early Mesolithic has largely been characterised by the investigations undertaken at Mount Sandel, Co. Londonderry. Here, numerous pits of varying sizes and a series of circular structures demarcated by post holes and sunken hearths were excavated (Woodman 1985; Bayliss and Woodman 2009). Based on these investigations, it is generally acknowledged that the Early Mesolithic commenced *ca.* 10,000 and lasted until *ca.* 9000 cal BP, whilst the subsequent Late Mesolithic took place between *ca.* 8500 and 6000 cal BP (Woodman 2015).

Despite a long-standing research history (>125 years), shell middens have largely been neglected within Irish archaeology (Milner and Woodman 2007; Woodman 2015). Whilst *ca.* 500 are known (with the majority being located in the northern half of the country (Woodman and Milner 2013), this is undoubtedly a serious underestimate of the overall true number. Owing to the scarcity of anthropogenic materials coupled with a lack of comprehensive AMS radiocarbon (^{14}C) dating, only a handful of shell middens have been securely assigned to the Mesolithic. Although the earliest shell middens date to the Late Mesolithic, *ca.* 7500 cal BP, the majority are dated to later periods, for instance the Neolithic to Iron Age shell midden at Culeenamore, Co. Sligo (Milner and Woodman 2007). At least 13 probable Mesolithic shell middens were identified by Milner & Woodman (2007), but several more have been identified and investigated since, for example at Tullybeg, Co. Galway (Murray 2009). The reasons for their infrequency are probably due to a number of factors, ranging from burial and/or erosion by marine transgressions since their formation to excavation for agricultural lime from the 19th century (Milner and Woodman 2007; Woodman and Milner 2013; Woodman 2015).

2. Materials and methods

2.1. Archaeological Context

The Conors Island shell midden sits on a low headland on Conors Island, Co. Sligo (**Figure 1**). Trial excavations led by Finbar McCormick took place in 2010. The site is a complex of small individual shell heaps, and has layers that have been assigned to the Mesolithic, Neolithic and Bronze Age periods. Since the Mesolithic part of the site was exposed in the cliff section (**Figure 1**), it was directly excavated via a test pit (Trench 4) measuring 1 × 1 m that closed down to 0.5 × 0.5 m. Although excavation was by single-context, all matrices were wet-sieved and floated to 0.25 mm to recover smaller classes of anthropogenic materials. The midden stratigraphy of Trench 4 consists of 5 individual layers, with the top layer (Layer 1) being a thin deposit of organic rich soil composed of sand with some clay and abundant rocks. This is followed by a shallow layer (Layer 2) of fine to medium sand, which included occasional oysters and cockles (*Cerastoderma edule*, Linnaeus, 1758). Layer 3 is principally composed of shell fragments (dominated by cockles followed by periwinkles (*Littorina littorea*, Linnaeus, 1758), oysters and limpets (*Patella* spp.) (**Figure 2**) within a compacted silty and clayey sand with some charcoal. Layer 4 yielded fewer remains but contained pockets of oyster and cockle shells (**Figure 2**), as well as charcoal fragments. The bottom layer (Layer 5) contained no shells and consisted of a brown sandy and compacted breccia with calcareous root tubuli and soft calcareous nodules. The oyster shells sampled in this study were derived from two contexts (5 and 7), identified as individual shell pockets, within Layer 4. Preliminary AMS radiocarbon (^{14}C) dating undertaken on two small roundwood charcoal samples from the base of the midden deposits in the cliff section adjacent to Trench 4, and equivalent to Layer 4 are provided in **Table 1**. When calibrated at 95.4% probability, these results yielded a Late Mesolithic age.

2.2. Methods

2.2.1. Determining Seasonality using Mg/Ca intensity ratios

Earlier evidence indicates that Mg/Ca ratios derived from mollusc carbonates cannot reliably produce absolute values for palaeo-temperatures, due to the physiological effects associated with the incorporation of Mg^{2+} into the shell carbonate (Lorrain et al., 2005; Wanamaker et al., 2008; Surge and Lohmann, 2008; Poulain et al., 2015; Graniero et al., 2017). These effects occur as Mg/Ca ratio offsets, that skew the Mg/Ca ratio on top of any seasonally changing patterns induced by environmental changes (see below). However, the degree to which superimposed physiological effects skew seasonal changes, can be species- or even specimen-specific and finding general correlations have been difficult to identify (Wanamaker et al. 2008; Graniero et al. 2017; Cobo et al. 2017; Hausmann et al. 2019a).

Oysters have a prominent role in Mg/Ca ratios as climate indicators and the published record on several oyster species (*Crassostrea virginica*, Gmelin, 1791, *Magallana*

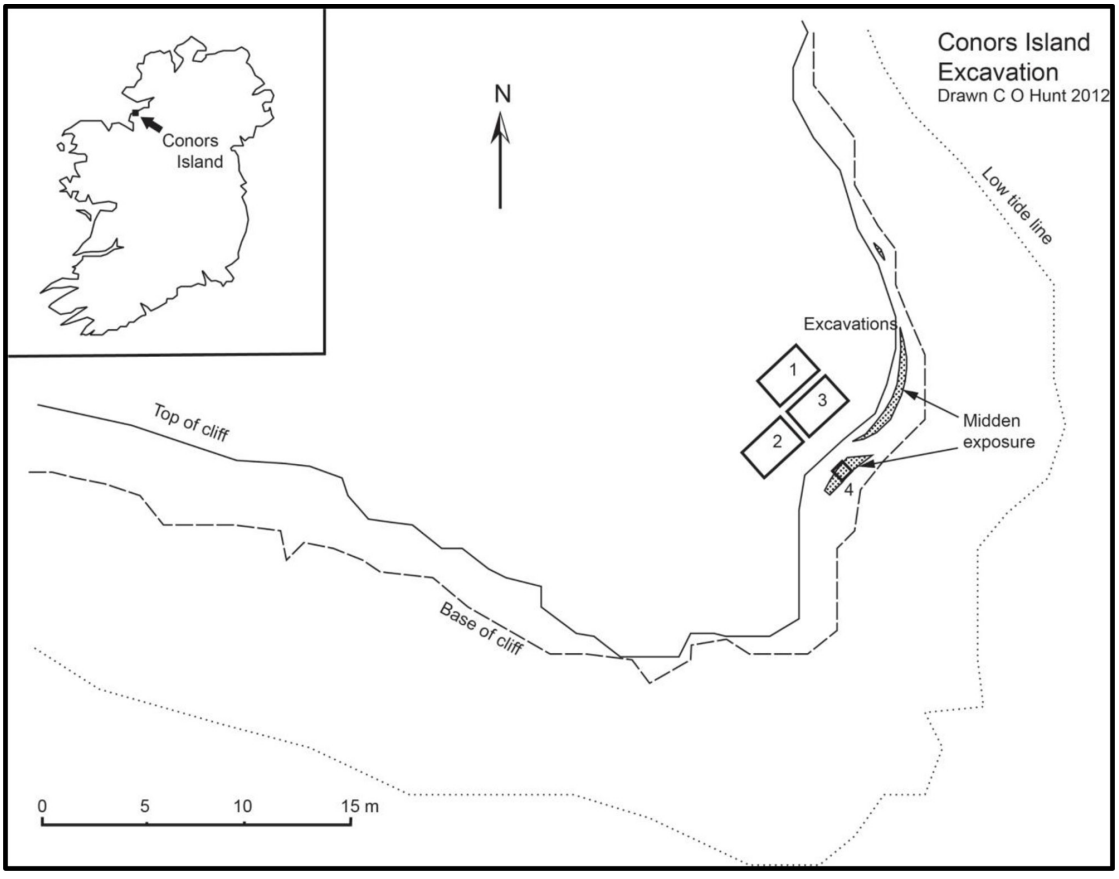

Figure 1: Plan of the Conors Island shell midden site. The molluscs in this study derive from two contexts (5 and 7) from Trench 4 located on the cliff. Insert shows the site in relation to Ireland.

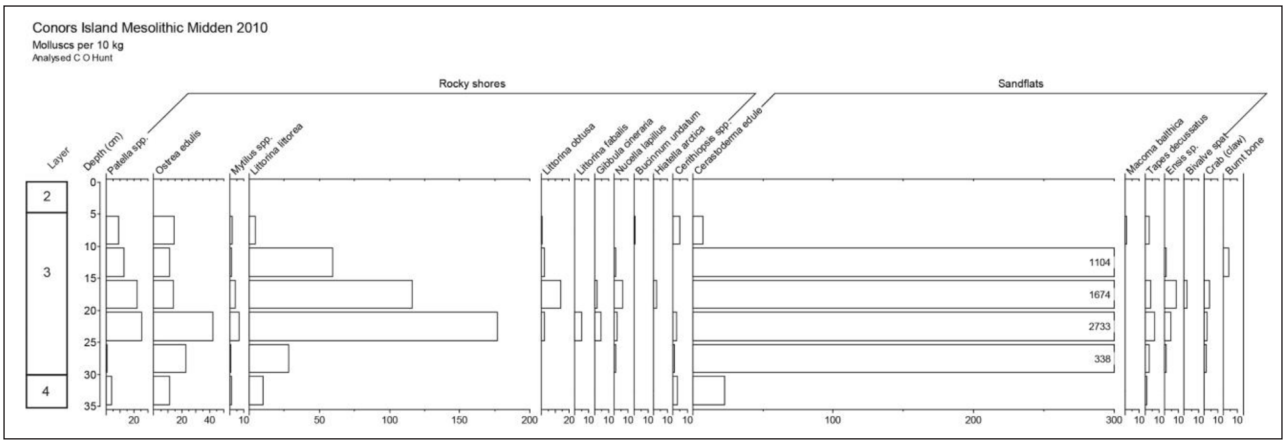

Figure 2: Number of Identified Specimens (NISP) per 10 kg of bulk sediment from the Conors Island Mesolithic midden. The dominant species at the Conors island midden are comparable with other Irish shell middens dating to the Mesolithic and Neolithic (Gutiérrez-Zugasti et al. 2011).

Table 1: Radiocarbon results on small roundwood charcoal from the cliff section adjacent to Trench 4, reported as conventional and calibrated years BP (95.4%) following Bronk Ramsey (Bronk Ramsey 2017). All dates were calibrated using the University of Oxford Radiocarbon Accelerator Unit programme OxCal (version 4.3.2), and the corresponding curve (IntCal13) for terrestrial samples (Reimer et al. 2013).

Sample ID	Laboratory Code	Radiocarbon Age (BP) ± error	Calibrated BP (95.4%)	Material	Species
Conors Is. 1.1	UBA-14433	5446 ± 27	6300–6200	charcoal	n/a
Conors Is. 1.6	UBA-14434	5403 ± 25	6290–6180	charcoal	n/a

gigas, Thunberg, 1793, *Ostrea* (*Turkostrea*) *strictiplicata,* Roulin and Delbos, 1855, and *Sokolowia buhsii*, Grewingk, 1853) shows that their seasonally changing Mg/Ca ratios, although not consistently correlating to palaeo-temperatures, reliably indicate annual growth patterns, individual growth rates, and individual ages of specimens (Bougeois et al. 2014; Bougeois et al. 2016; Durham et al. 2017). In these species, growth rates generally had lower Mg/Ca ratios in periods of slow growth and higher Mg/Ca ratios in periods of faster growth. To what degree these growth patterns also happen parallel to seasonal changes in temperature is unclear and likely locality specific (Mouchi et al. 2013). However, in temperate climates with distinct seasonal temperature changes that reach below 10°C (Kirby et al. 1998), it is common for oysters to stop growing altogether, resulting in distinct incremental growth patterns indicating annual cessations in growth (Milner 2002; Robson 2015), which are also rich in organic material that increases the Mg/Ca ratios (Schöne et al. 2010).

Based on the aforementioned information, to determine the Conors Island oysters' individual biological age and season of death, we expected the following: (a) growth rates cease annually during the colder months of the year (Bougeois et al. 2014; Bougeois et al. 2016; Durham et al. 2017), i.e. winter, resulting in an annual growth-line (Milner 2002; Robson 2015) with a high Mg/Ca ratio (Schöne et al. 2010), and (b) growth will be the fastest (resulting in a higher Mg/Ca ratio) during the warmer months of the year, i.e. summer, (Mouchi et al. 2013; Durham et al. 2017) and lowest immediately before and just after annual growth ceases in the winter (yielding a lower Mg/Ca ratio just before and after growth-lines).

2.2.2. Inhibiting factors for determining seasonality using Mg/Ca ratios

Besides the connection between Mg/Ca ratios and growth rates, there are further factors influencing the elemental composition (Elliot et al. 2009; Freitas et al. 2012; Poulain et al. 2015; Hausmann et al. 2017). These additional factors have the potential to superimpose seasonal patterns of growth, and thus frustrate the interpretation of the season of death. Most prominently, these additional factors have been identified as the following: (1) gradual change of the Mg/Ca ratios with increasing distance to the hinge (Hausmann et al. 2017), (2) age-related (ontogenetic) baseline shifts of Mg/Ca ratios (Elliot 2009), and, (3) short-lived peaks of high Mg/Ca ratios during unpredicted growth cessations leading to organically rich lines (Schöne et al. 2013), which are additional to the predicted annual growth cessation. By mapping the entirety of the hinge section (**Figure 3a**), we aim to assess the spatial impact of these factors across the growth increments and find ways to avoid or acknowledge them in our interpretation of growth patterns.

Gradual increases or inconsistent Mg/Ca ratios towards the exterior shell edge or hinge have been identified in *Pecten maximus* (Linnaeus, 1758) (Freitas et al. 2012), *Ostrea edulis* (Linnaeus, 1758) (Hausmann et al. 2017), *Arctica islandica* (Linnaeus, 1767) (Schöne et al. 2013) and *Ruditapes philippinarum* (A. Adams & Reeve, 1850) (Poulain et al. 2015). In these cases Mg/Ca ratios were

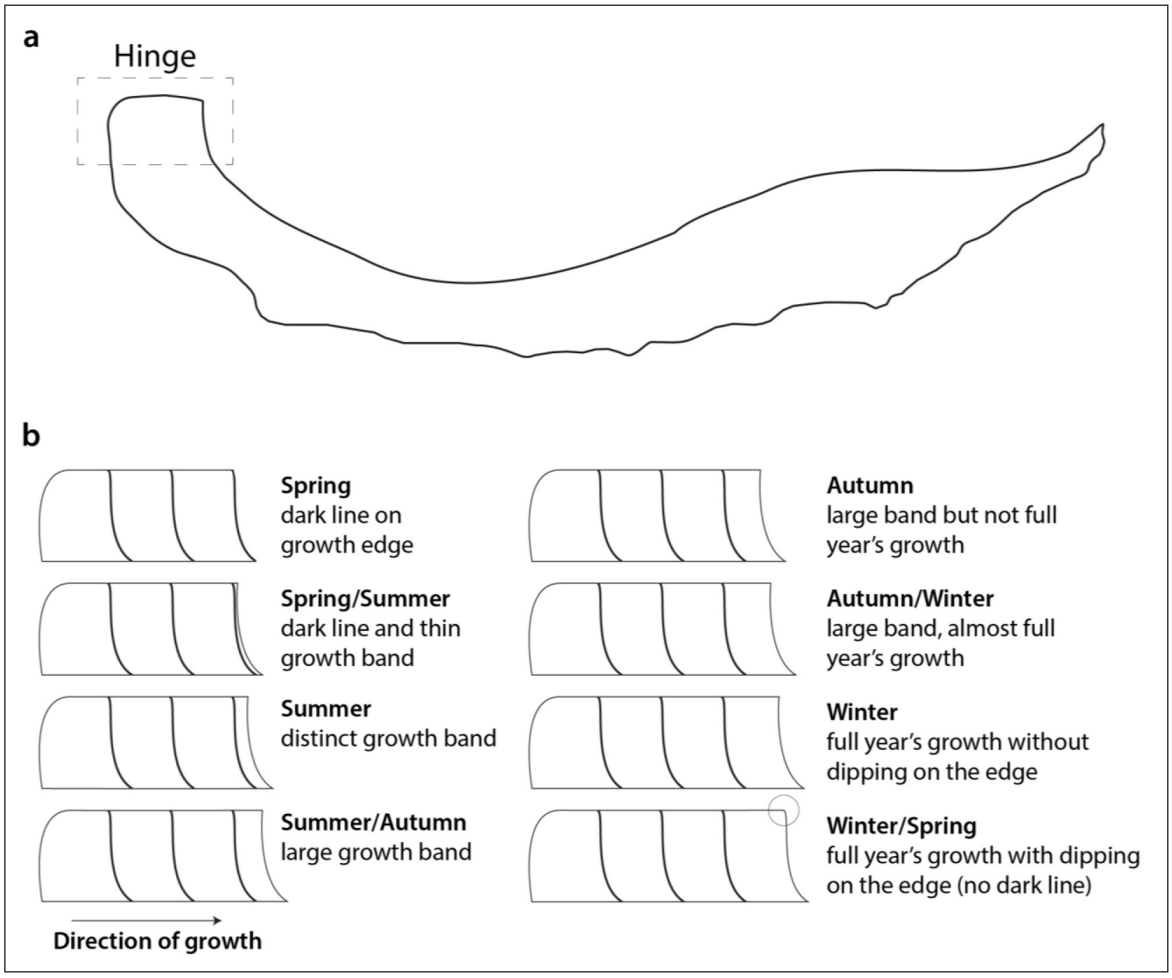

Figure 3: (a) Hinge location on an oyster shell thin-section, and **(b)** ideal seasonal succession of growth patterns as defined in Robson (2015).

inconsistent within growth increments, resulting in an increased variability of elemental ranges between specimens and unclear seasonality records, where annual minima were less distinct as the baseline increased. Contrary to the above, Durham et al. (2017) produced evidence for *C. virginica* shells that, if at all, the opposite was true and that Mg/Ca ratios slightly decrease towards the exterior shell edge ($R^2 = 0.05$; $p \leq 0.0001$). Spatially extensive elemental mapping should provide the means to reveal these patterns, should they occur.

Ontogenetic trends have also been revealed in a range of elemental records of shell specimens (Gillikin et al. 2005; Ford et al. 2010; Schöne et al. 2011). These trends were expressed as gradual shifts in the baseline, which obscured annual minima and maxima, the cornerstone of annual growth patterns, and made it difficult to differentiate them from random irregularities of the record. While 2D maps will experience the same ontogenetic offsets as simple linear scans, it is easier to account for irregularities within the record and find ways to make annual minima and maxima more distinct from them.

Lastly, the impact of organic material occurring within the shell is unavoidable, when measuring *in situ* (Schöne et al. 2013; García-Escárzaga et al. 2018). As such, the Mg/Ca ratio measured through LIBS always consists of the carbonate component as well as the insoluble organic matrix (IOM) of the shell. While the IOM is usually not abundant enough to skew the Mg/Ca ratio of the carbonate record, it can be found amply within annual growth-lines. These growth-lines then produce high Mg/Ca ratios, while the Mg/Ca ratio of the carbonate component remains the same. This pattern is most visible in growth-lines that predictably occur in winter growth cessations, which are preceded by a slower period of growth and a lower Mg/Ca ratio. Thus, growth-lines occur as distinct peaks during lower Mg/Ca ratio periods. Through mapping, we expect these lines to be even more distinct (i.e. lines instead of rounded peaks) and provide guides for the general growth structures of the shells.

2.2.3. Sample preparation for Laser Induced Breakdown Spectroscopy

We followed the methodology for Mg/Ca mapping developed by (Hausmann et al. 2019a), in which a full step-by-step guide is deposited on the protocols.io repository (Hausmann et al. 2019c). The oyster shells were sectioned using a Buehler ISOMET 1000 Precision Saw (Model 11-2180), and a Buehler Diamond Wafering Blade (Series 15LC Diamond No 11-4276). The section followed the direction of growth and covered the entire hinge towards the growth edge. Since the cutting procedure yielded two halves, the better-sectioned (i.e. no fractures) half

was selected for analysis and subsequently cleaned with ethanol to remove any residue. The shells were then put into a holder made of aluminium-foil to vaguely position the section in a levelled horizontal position under the focusing lens. The actual xyz-orientation of the sample surface was determined by 3 surface points that were manually focused on and share an xyz-plane, which builds the foundation of the 2D map. We then determined the limits of the sample surface on the x- and y-axes. Within these limits we automatically generated a point mesh of 75 μm or 100 μm resolution, depending on the sample requirements. Based on this point mesh, data acquisition was carried out with each point being measured 5 times to accumulate an averaged spectrum. While accumulated spectra do not allow to assess variability between each measurement, we measured the variability in an additional line scan, where each of the 5 spectra were analysed separately. Their variability had a relative standard deviation of 7.4 ± 3.3%. After each point, the averaged Mg/Ca ratio was automatically associated with the coordinates of that point, resulting in a 2D map of the Mg/Ca ratios.

2.2.4. Laser Induced Breakdown Spectroscopy instrumentation

We employed a Q-switched Nd:YAG laser (Spectron Laser Systems), operating at the fundamental wavelength (1064 nm) and producing 10 ns pulses with a pulse energy of ~10 mJ in our analysis. Using a quartz lens of 28 mm focal length, the laser beam was focused onto the sample surface. The focal point of the lens was set slightly below the sample surface, and the working distance (focusing lens-to-sample distance) was adjusted so that a crater with a diameter of about 50 μm was measured on ablated spots performed directly on the sample.

The sample was mounted on an xyz-motorised micrometer stage and a CCD camera (Point Grey Grasshopper 3) was placed in vertical alignment with the sample surface. Thus, a clear image of the sampling area was visible through the camera at an optical magnification of ~4:1. This magnification was a necessary compromise to achieve a general overview of the shell as well as good visibility of the growth increments.

Measurements were performed at room temperature. The light emitted by the plasma plume was collected by an optical fiber and transmitted to a Czerny-Turner spectrograph (Jobin Yvon, TRIAX 320) for analysis in conjunction with an intensified charge coupled device (ICCD) detector (DH520-18F, Andor Technology). The spectrograph was equipped with a 600 grooves/mm grating providing a spectral resolution of about 0.1 nm and a spectral range of 80 nm. The ICCD is gated by means of a digital delay pulse generator (DG535, Stanford Research Systems) and synchronised to the Q-switch of the laser.

Spectra were acquired 0.5 μs after the firing of the laser pulse with an integration time of 1 μs, based on the acquisition parameters performed in Hausmann et al. (2017) using standards developed by Cobo et al. (2017), which revealed that both Mg and Ca emission lines had sufficient intensity, a high signal to noise value, and provided an accurate representation of the mole ratio of both elements ($R > 0.99$, $p < 0.01$). The emission lines providing the most reliable Mg/Ca ratio were Ca II ($^2D_{3/2} \rightarrow {}^2P_{1/2}$) emission line at 315.887 nm and the Mg II ($^2P_{3/2} \rightarrow {}^2S_{1/2}$) at 279.553 nm. Therefore, a spectral range centered around 300 nm was selected to record the LIBS spectra.

2.2.5 Sample preparation for incremental growth-line analysis

To undertake the incremental growth-line analysis, the oysters were thin-sectioned using the method developed by Milner (2001) with some modifications, which have also been deposited as a step-by-step guide on protocols.io (Hausmann et al. 2019d). Following the elemental mapping, the sectioned shells were placed face down in 1- and 2-inch plastic moulds respectively depending upon the size of the cut hinge. The plastic moulds had been cleaned with alcohol and then rinsed with water, left to dry, and coated with Buehler Release Agent No 20-8185-016. The hinges were embedded in resin (2 parts by volume of Buehler Epo-Thin Low Viscosity Epoxy Resin No 20-8140-12B mixed with 1 part by volume Buehler Epo-Thin Low Viscosity Epoxy Hardener No 20-8142-016), and left to cure in an environment of constant humidity and temperature overnight. Once hardened, the resin blocks were removed from the moulds and labelled. The resin blocks were then lightly ground using successively finer metallographic grit papers (P600, P1200 and P2500 grades respectively) on a Buehler Motopol 2000 Grinder/Polisher. The surfaces of the resin blocks were cleaned with water and left to dry. Then, they were polished using a Texmet polishing cloth coated in Buehler MetaDi 3 μm water based diamond paste, rinsed with water and left to dry overnight. The polished facets of the resin blocks were attached to a glass slide using Loctite 322 Adhesive, exposed to an ultraviolet light source and left to harden for 24 hours. Once the sample had bonded to the slide, the bodies of the resin blocks were cut from the slide using a Buehler ISOMET 1000 Precision Saw, thus leaving a slice of the embedded hinge of approximately 200 to 500 μm in thickness on the glass slide. In order to clearly see the microstructure of the shell, the shell and resin were lightly ground to produce the thin section. The slide was placed in a slide holder and held face down over revolving grit papers (as detailed above) until the final thinness (<50 μm) was achieved. This varied from sample to sample, and was monitored by eye as well as repeated checks under a light microscope. Lastly, the sample was polished on a Texmet polishing cloth with Buehler MetaDi 3 μm water based diamond paste.

The thin sections were examined at magnifications between ×10 and ×40. The annual lines were noted for each shell and counted; any other lines, for instance cessations in growth, were recorded, and the last section of growth (from the last line to the outer edge) was examined in order to assess the season of death using the criteria shown in **Table 2** and illustrated in **Figure 3b**. Since the initial method development (Milner 2001), interpretations have, however, altered. Originally, a month was assigned to each shell but this caveat had a margin or error of ±1 month (Milner 2001, 2002). Thus, in more

Table 2: Table to show the identifications and assignments to particular seasons starting with line formation in the spring (Robson 2015) (See also Figure 3b).

Season	Identification
Spring	A line is present right on the edge and the edge dips down
Spring/summer	Shell shows a new line and a very thin band of new growth
Summer	Band of growth between the last annual line and the shell edge
Summer/autumn	Large band of growth between the last annual line and the shell edge and a spawning line may be present
Autumn	Large band of growth but not a full year
Autumn/winter	Large band of growth – almost a fully year
Winter	Large band of growth which looks like a full year but no dipping on the edge
Winter/spring	Darkening of growth edge begins and dipping downwards on the edge

recent analysis (e.g. Robson 2015) a seasonal assessment has been made. It is felt that seasons are more representative because they remove the false perception that interpretations are accurate to within a month and take into account the margin of error. However, they have also been subdivided into split seasons.

In addition, the confidence in the season varied. The highest degree of confidence was assigned to shells with a line directly on the edge indicating line formation, and a spring death (March or April). This was because the line is a clear indicator. However, from the modern control study (Milner 2002), it was clear that line formation did not occur on one day. There was variation within a population, and therefore a sample of oysters collected on one day may include oysters with lines and oysters without. This sample would be interpreted as having winter/spring and spring oysters. Thus, it is important to note that such a grouping may not indicate two seasons but possibly one collection event (Robson 2015). Oysters gathered during the spring/summer (*ca.* May, June), and summer (*ca.* July, August) were equally easily interpreted because their lines are close to the edge and may also include a spawning line. However, from October onwards, growth reduced significantly. Generally it is possible to identify an oyster harvested during the autumn (*ca.* September, October), because there does not appear to be a full years growth. However, distinguishing between oysters harvested during the autumn/winter (*ca.* October, November), winter (*ca.* December, January), and winter/spring (*ca.* February, March) was mostchallenging since the only indicator was the topography at the top of the shell that started to dip down when a line was due to form (Milner 2002; Robson 2015).

3. Results

3.1. Elemental analysis

The Mg/Ca ratios of the 12 specimens were mapped (**Figure 4**) producing variable results in terms of the overall ranges of Mg/Ca ratios as well as the visibility of seasonal patterns (**Table 3**). The quantity of sample points ranged from 3,497 points (sample 7E) to 8,847 points (sample 5G), depending on the size of the specimen and the applied sampling resolution (75 or 100 μm depending on visibility).

The ranges of the Mg/Ca ratios also varied between specimens, but generally the values were between 0.03 and 0.20. That being said, each map contained some outliers (e.g. along the hinges) that exceeded these values and reached maxima of 0.63 (sample 5A) and 0.66 (sample 7E).

3.2. Mg/Ca annual patterns

Repeating annual patterns of Mg/Ca ratios were visible across complete increments in almost all specimens. Specifically, two annual patterns occurred in the majority of the specimens (**Figure 5**): (1) a gradual increase and subsequent decrease of Mg/Ca ratios across whole growth increments is in agreement with earlier conclusions that Mg/Ca ratios correlate with changes in growth rate (**Figure 5a**) (e.g. Durham et al 2017), and (2) a thin but distinct line with high Mg/Ca ratios consistent with annual growth lines during a growth stop (**Figure 6b**) (Schöne et al. 2013). Both patterns were found with variable clarity in the individual maps underlining their specimen specific nature.

Overall, we discerned the biological age for 9/12 (75%) specimens and the season of death for 11/12 (92%) specimens. Ages ranged between 2 and 7 years and averaged ~4 years. Specimens that did not produce a clear biological age, still produced an age of ±1 year (i.e. '4 or 5 years' and '5 or 6 years').

We further determined the specimens' season of death: 2 × spring, 2 × spring/summer, 1 × summer, 2 × autumn, 1 × autumn/winter, 3 × winter (and 1 × unclear). There was some overlap in the specimens that did not produce a clear biological age and no clear season of death, however as the season of death is only determined by the last year of growth, any anomalies and unclear growth patterns that would have affected previous years, and thus the interpretation of the biological age, would not necessarily affect the interpretation of the season of death.

Ultimately, these results are predominantly useful for assessing the visibility of growth patterns in elemental maps, but offer a rather narrow statistical basis for making deductions about seasonal prehistoric exploitation patterns, given the small sample size.

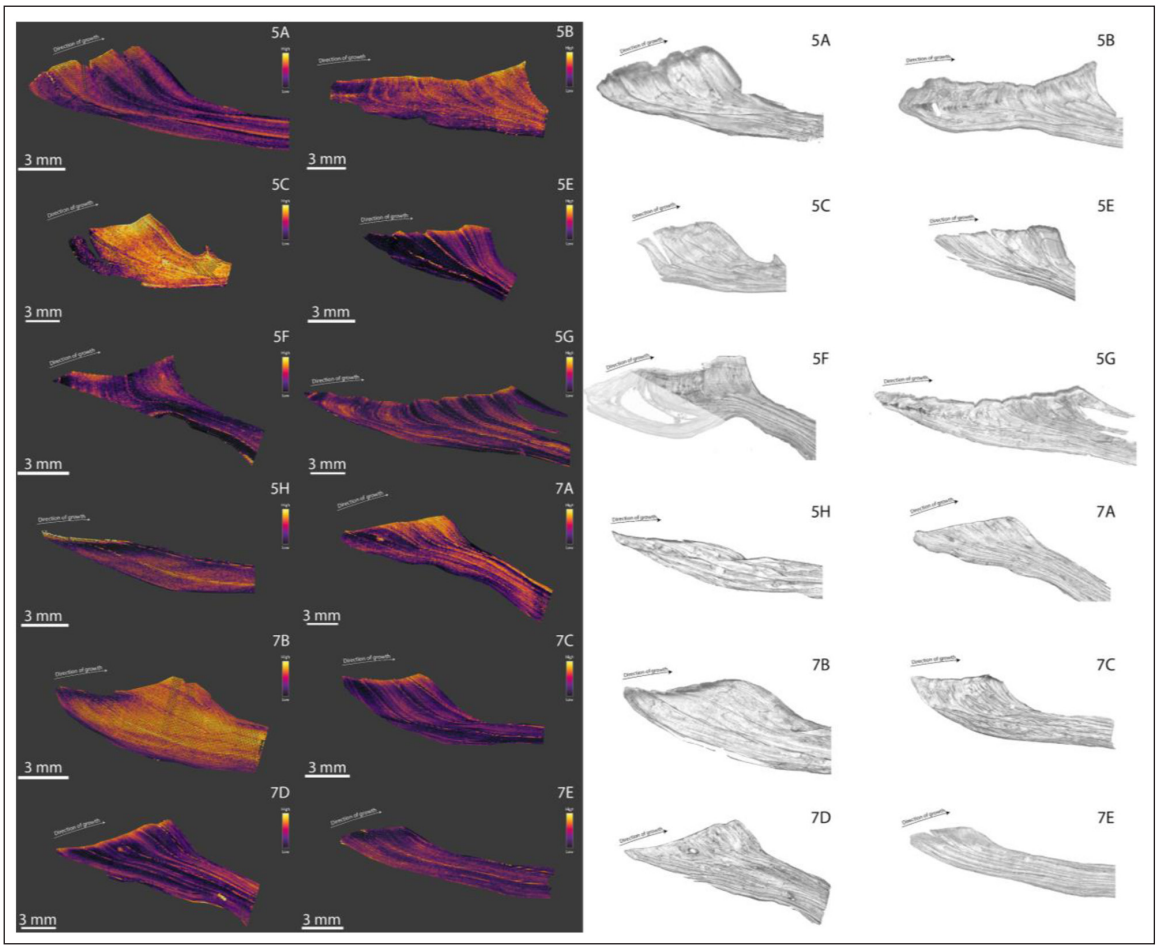

Figure 4: Elemental maps and growth micro-images of the oyster shell thin sections. Samples are in order of their stratigraphic layer and grouped by method. The scales shown for the elemental maps are also applicable to the mico-images. Note that the colouring of the elemental maps is based on the individual limits of each specimen's Mg/Ca ratio, with bright colours showing high ratios and dark colours showing low ratios.

3.3. Mg/Ca spatial variations and physiological effects

The annual banding of Mg/Ca ratios was often least obvious at the very edge of the hinge of the shell, where the range of Mg/Ca ratios between gradual increases and decreases was usually the lowest. This was due to intra-incremental increases of the Mg/Ca ratios towards the hinge. We exemplified this increase by measuring the change in Mg/Ca ratios along single growth increments and during the maximum time of growth in three years each (arbitrarily named A, B and C) for two specimens, 5A and 7A (**Figure 6**). Within each increment, Mg/Ca ratios dropped with increasing distance to the hinge. In specimen 5A, this decrease was from 0.18 at the hinge to 0.08 at a 5 mm distance, and in specimen 7A from ~0.17 to 0.08 after 5 mm. While the Mg/Ca ratios of each year converge into similar ratios with increasing distance, the variability of ratios at the very hinge was more pronounced, suggesting that there are further variations between each year. In contrast to the increased ratios in specimens 5A and 7A, there were also instances when Mg/Ca ratios were lower at the hinge and rose with increasing distance (see 5H, 7B and 7E in **Figure 4**), mirroring earlier finds by Durham et al. (2017).

3.4. Ontogenetic trends in Mg/Ca ratios

We found a variety of ontogenetic changes in the Mg/Ca ratios. Firstly, a gradual increase with increasing age in specimens 7A and 5B. This trend mirrors the results of other studies (Elliot et al. 2009; Ford et al. 2010; Mouchi et al. 2013) but was not consistent in all specimens (e.g. 5A, 5G, 5H, 7E).

The second ontogenetic trend showed abrupt (instead of gradual) baseline increases of Mg/Ca ratios after one or two years of growth in specimens 5A, 5E, 7A and 7C, which was preceded by a lack in the seasonal patterns of the Mg/Ca ratios entirely (**Figure 4**, see also **Figure 5b**). Instead, there was little variation in the Mg/Ca ratios for this preceding period, and were only interrupted by distinct high Mg/Ca ratio growth lines, that are likely high in organic material.

Thirdly, a combination of hinge-specific Mg/Ca ratio variations and ontogenetic trends was found in specimens 5C, 7E and 7B. Their near-hinge parts were consistently low in Mg/Ca ratios during the first two years of growth.

3.5. Incremental growth-line analysis

The microscopic analysis of the incremental growth-lines produced some results that corresponded with the elemental analysis of the spatial patterns in the Mg/Ca

Table 3: General description of the LIBS generated elemental maps, their indication of biological age and the occurrence of ontogenetic trends, as well as the results obtained from incremental growth-line analysis. Visibility of seasonal patterns in Mg/Ca maps is described as very clear: ++, clear: +, moderate: O, and unclear: –.

Specimen	N	Res	Length [mm]	Min	Max	LIBS-Analysis				Incremental Growth Analysis	
						Visibility of seasonal pattern	Ontogenetic trends	Age [a]	Season of death	Age [a]	Season of death
5A	6,392	100	7.5	0.03	**0.63**	++		4	Winter	4	Summer
5B	5,634	100	15.2	0.04	0.33	–	Yes	4 or 5	/	Unread-able	Unread-able
5C	5,755	100	6.8	0.03	0.44	O	Yes	4 or 5	Spring	4	Autumn/ winter
5E	4,388	**75**	6.9	0.03	0.5	+	Yes	4	Autumn/ winter	4	Spring/ summer
5F	7,840	**75**	7.3*	0.04	0.35	+	Yes	2	Winter	3	Winter
5G	**8,847**	100	18.7	0.04	0.47	+	No	6	Winter	5	Spring/ summer
5H	4,084	100	5	0.04	0.44	++	No	2	Spring	2	Spring/ summer
7A	7,761	100	10.5	0.03	0.36	++	Yes	6	Autumn	10	Autumn/ winter
7B	7,842	**75**	7.6	0.05	0.29	O	Yes	3	Spring/ summer	3	Autumn/ winter
7C	5,822	**75**	5.4	0.05	0.18	+	Yes	5	Autumn	Unread-able	Unread-able
7D	6,798	100	10.3	0.04	0.33	–	No	5 or 6	Spring/ summer	10	Summer
7E	**3,497**	100	4.7	0.05	**0.66**	+	No	2	Spring	2	Spring

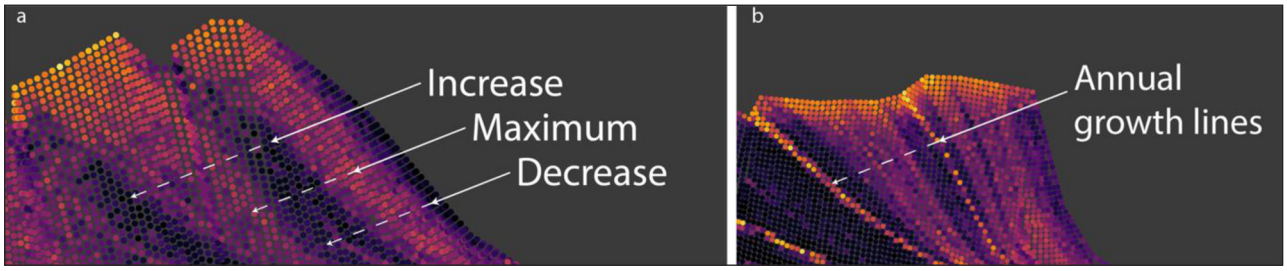

Figure 5: Examples for patterns found in most of the Mg/Ca maps. See Figure 5 for description of colours. **(a)** Gradually changing Mg/Ca ratios of specimen 5A with an annual increase, maximum and subsequent decrease. **(b)** Thin lines with high Mg/Ca ratios that occur in areas of specimen 5E with low Mg/Ca ratios, separating annual growth intervals. Also note the low values and little variation of Mg/Ca ratios in preceding years in specimen 5E.

ratios (50% of the readable thin sections). Specifically, the biological ages as determined by the growth increments ranged from 2 to 10 years. This is a broader range than what was determined using the elemental maps (2 to 7 years). With one exception (5G), growth increments produced greater biological ages than elemental maps, with an average of ~4.7 years. This was likely caused by irregular growth lines evident in the micrographs that suggested additional years of age.

Moreover, 5/10 (50%) determined seasons of death were different compared to the results from the elemental mapping. Whilst some of the differences were minor (i.e. autumn/winter instead of autumn) or in areas where seasonal differences are minute (i.e. in periods of slow growth), some differences were major (e.g. 5A) and the season of death was entirely different (summer instead of winter) than the elemental maps. These deviating specimens and our interpretations why they produced different results are found below (section 4.1).

Lastly, one shell specimen (7C) was unsuccessful in providing an age or season of death, because its growth edge had broken off during the preparation process. In

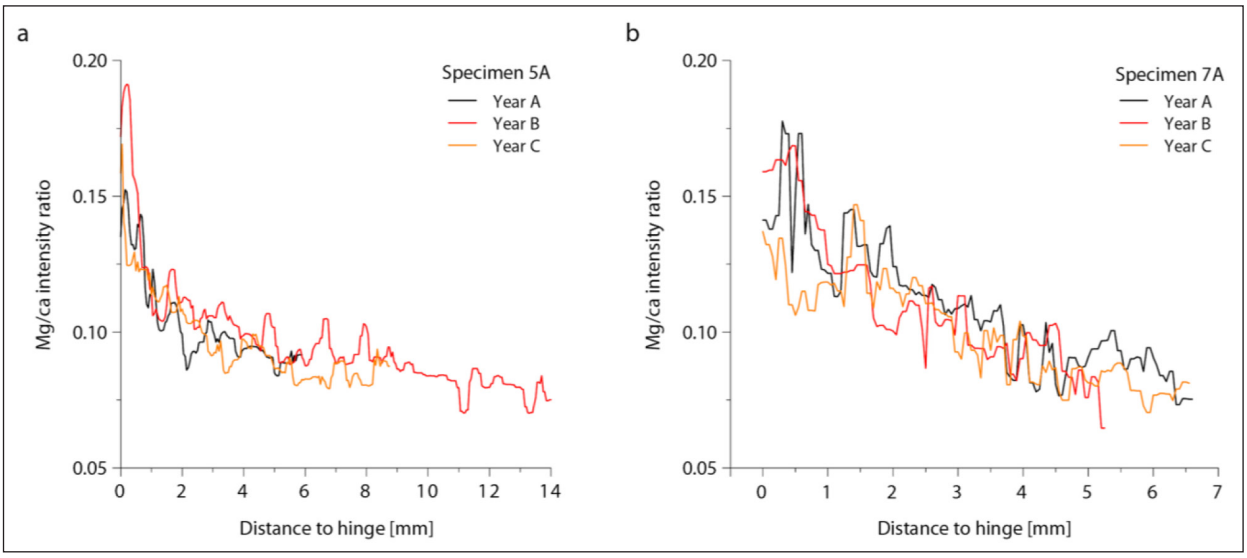

Figure 6: Comparison of line scans that depict the variation of Mg/Ca ratios within single growth increments and perpendicular to the direction of growth in three years of specimens 5A and 7A. Mg/Ca ratios at the very edge of the hinge are higher than ratios in the isochronous parts that are farther from the hinge. Note that the three years from each shell are not the same years as shells are likely not coeval.

addition, sample 5B could not provide a conclusive result due to its very complex growth structure. Overall, 2/12 (16.6%) specimens did not yield any data on biological age or season of death.

4. Discussion

4.1. Deviations in the seasons of death between the two methods

Whilst the data obtained from both methods suggest multi-seasonal shellfish exploitation and site occupation, it is important to note why, in several cases, the results deviate from one another. In the following, we discuss the rationale for the deviating five samples.

5A – Both methods showed 4 years of age at death, however the season of death was indicated as winter by the elemental mapping and summer by the incremental growth-line analysis. The reason for this divergence was the comparatively short growth rate in the final year, which is evident in the gradual decrease of the Mg/Ca ratios towards the edge. However, in the incremental growth-line analysis, in which the size of the annual increments is an indication for how much time has passed since the last major growth line, the decrease in the growth rate was not evident and the final annual growth increment appeared as though it had only partially grown (see also **Figure 3b** for summer and winter thickness).

5C – Despite both methods yielding a clear biological age of ~4 years at death, it was difficult to confidently assess the season of death. Given the irregular growth patterning we were unable to confidently compare the final with the preceding annual increments. Moreover, the map of the Mg/Ca ratios was very noisy making interpretation problematic. This resulted in two diverging interpretations regarding the thickness of each annual growth increment, and thus divergent assignations for the final annual increment in terms of where in the growth cycle it stopped.

5E – While the elemental map showed clear organic-rich annual banding, the micrograph of the thin-section suffered some breakage, likely due to over-polishing. This potentially resulted in a misleading line suggesting an additional growth cessation, and thus a reduced band of growth since the previous annual line. This reduction indicated an earlier season, in this case spring.

5G – Although the micrograph of the thin section appeared to display distinct banding, which may have been accentuated by air pockets, the Mg/Ca maps differed, and clearly show organic rich growth-lines with gradual changes in the Mg/Ca ratios.

7B – The micrograph indicated that some substantial growth had taken place since the previous annual cessation, which would correspond to a full year's growth. As such the season of death was interpreted as autumn/winter. However, comparison with the map of the Mg/Ca ratios indicated that the most recent portion of the hinge had been lost during the manufacturing process, meaning that a proportion of the year was missing.

The aforementioned results show the complexities involved in the interpretation of maps of Mg/Ca ratios within and between oyster shells. While no singular factor (i.e. growth rates) influencing the Mg/Ca ratios was present in every specimen, the elemental maps provide an insight into the multitude of spatial and temporal patterns that are encountered in tandem with growth related expressions of Mg/Ca ratios. To these expressions, the incremental growth-line analysis of thin sections has provided a valuable context. Most notably, there is some overlap between the annual growth-lines found within the thin sections and lines that are high in Mg/Ca ratios, mirroring earlier results (Schöne et al. 2010; Hausmann et al. 2017). Further, where annual patterns were less visible in the LIBS generated elemental maps, thin sections, while not providing an explanation for the elemental patterns, still exhibited growth structures with undisturbed

quality, providing an additional record to compare our geochemical data with. However, when the incremental growth-line records were interpreted on their own, the results often deviated from the outcome of the elemental analysis (**Table 3**). While there is a degree of subjectivity in determining the seasons of death, we argue that the main reason for these deviations are irregular growth lines (also termed disturbance lines). These lines often form unpredictably throughout the year as a result of spawning, predator attacks and/or storms (Andrus and Crowe 2000; Surge et al. 2001; Durham et al. 2017). We are also conscious of the experience of the analyst resulting in the misidentification of the season of death and/or years of growth. While these lines can be difficult to identify under the microscope, maps of Mg/Ca ratios generally differentiate between annual and irregular lines, because genuine annual lines (high in Mg/Ca ratio) are often found in areas of slow-growth (low-Mg/Ca ratio) (**Figure 7**). We are thus in agreement with other studies that compared geochemical and structural information of oysters (Andrus and Crowe 2000; Surge et al. 2001; Durham et al. 2017), and argue that incremental growth-line data can be unreliable on its own, but can provide valuable information to contextualise the geochemical data.

4.2. Intra-specimen and intra-increment variability in Mg/Ca

Recent work including extensive elemental mapping of a larger set of molluscs has revealed variability of the Mg/Ca ratios between and within specimens (Hausmann et al. 2019a). While their study was focused on the Mediterranean limpet (*Patella caerulea*, Linnaeus, 1758), there are some similarities with the variation of the elemental maps identified in the oyster of this study. Foremost, the spatial inconsistency of Mg/Ca ratios along single growth increments is troublesome in terms of connecting Mg/Ca ratios to changes over time. As growth increments are traditionally thought to represent growth conditions at a certain point (or period) in time, their elemental composition should also represent these conditions. However, the wide range of Mg/Ca ratios found within single growth increments, indicates that isolated elemental ratios are difficult to simply translate into specific growth conditions or environmental parameters (e.g. sea surface temperature) as in the case of *P. caerulea* (Ferguson et al. 2011; Hausmann et al. 2019a). Specifically, because Mg/Ca ratios can vary depending on the distance to the shell hinge, it is not always possible to acquire definitive absolute ratios. Consequently, any measured ratio will have to be interpreted in relation to the rest of the increment and the rest of the record. This restriction, to some degree, also extends the comparison of the Mg/Ca ratios between specimens, because the patterns of spatial variability of the Mg/Ca ratios are not expressed consistently enough to generalise between specimens. Thus, Mg/Ca ratio variability cannot reliably be avoided by for example sampling at an equal distance to the hinge. Further, interpretations that imply environment specific or species specific influences on the Mg/Ca ranges based on line scans need to verify these influences using 2D mapping (Bougeois et al. 2016; Mouchi et al. 2018).

Ultimately, these differences do not only illustrate the need to map elemental ratios over line scans, but also the need for increased sample sizes that accurately depict the wider variability of the spatial patterning of elemental ratios. Our preliminary dataset on Irish oyster shells provides the foundation for future analyses employing LIBS as a means to generate fast 2D maps of shell sections. Limited by the 10Hz Nd:YAG laser, our sampling speed was lower compared with other LIBS systems, which employed 100Hz (Cáceres et al. 2017) or 1,000 Hz lasers (Rifai et al. 2018) and acquired geochemical maps with the dimensions used in our study within <5 min. Thus, the time for elemental analysis does not exceed the time for sample preparation (i.e. sectioning), shifting the practical constraints of analysing large shell assemblages away from the geochemical analysis.

4.3. Access to large shell assemblages

The ability to access geochemical records in a large quantity of shells, has implications for archaeological and palaeoecological studies. For archaeology, increased sample sizes would improve the robustness and detail of seasonality studies, a problem more thoroughly described by West et al. (2018). In particular, through increased sample sizes, it is possible to further analyse previously ignored stratigraphic contexts or layers, and expand the analysis of previous layers to many more shell specimens.

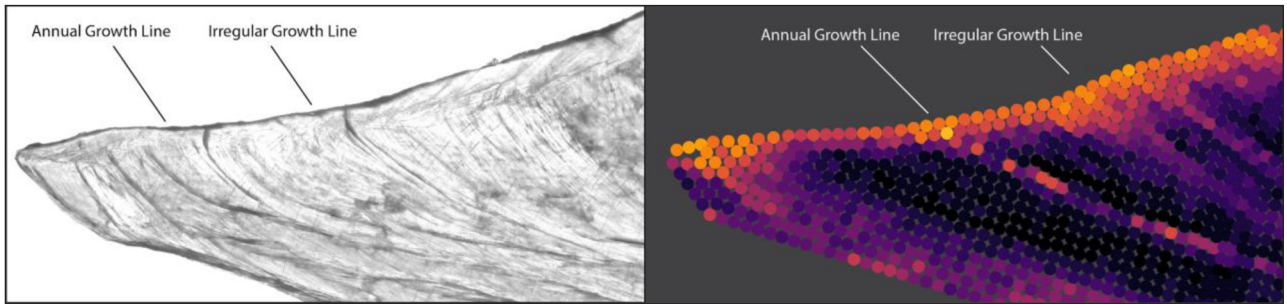

Figure 7: Regular annual and irregular growth lines as they are visible under the microscope (left) and in an elemental map (right). Differentiating between both kinds of lines under the microscope is often difficult, which can result in the misinterpretation of the season of capture. Elemental maps are more suited for making this distinction because they also depict growth reductions that precede and follow true annual growth lines. See Figure 4 for description of colours and full view of the specimen (7D).

This has been argued to increase stratigraphic resolution, providing a seasonal component and an estimate of variability between different areas of one site (Robson 2015; Hausmann and Meredith-Williams 2017b), or between closely related sites within a landscape (West et al. 2018), and lastly to provide a close up of depositional activities and ritual contexts (Thompson and Andrus 2011).

For palaeoecological research, oysters have provided baselines for primary productivity and regional variability of marine habitats in a range of contexts (Grabowski and Powers 2004; Rick and Lockwood 2013; Baggett et al. 2015; Savarese et al. 2016; Rick et al. 2016). When possible, measurements of size and of biological age were used to assess changes in environmental conditions as well as changes in human exploitation (Gutiérrez-Zugasti 2011). However, due to the difficulties of assessing biological age for a large number of specimens, it is generally not feasible to go beyond size measurements for spatially and chronologically extensive studies (Rick et al. 2016). This prevents researchers from quantifying the differential impact that environmental and anthropogenic changes can have on shellfish populations (Mannino and Thomas 2001, 2002). To fully understand the causes behind oyster population changes and the best means to sustain current populations, it is key to differentiate between these factors. Fast elemental mapping thus represents a crucial tool for expanding current age/size datasets of modern as well as ancient oyster populations.

4.4. Seasonal exploitation patterns at Conors Island and during the Irish Mesolithic

Following the elemental mapping of the Mg/Ca ratios, the small assemblage analysed here demonstrates that oyster collection at Conors Island occurred throughout the majority of the year. Moreover, these initial data are congruent with preliminary $\delta^{18}O$ stable isotope analysis undertaken on oysters from the same layer (Layer 4) of the site, which similarly demonstrated that oysters were collected on several occasions throughout the year with the exclusion of summer (S. Neill personal communication). Despite the small sample size, oysters were targeted throughout the year, with the exception of summer and winter in Contexts 5 and 7 respectively. Further work is required on a larger sample of oysters from both contexts (as well as layers) though the reasons for these differences may be related to economic, environmental, cultural and/or social practices (Rowley-Conwy 1984, 2002; Milner 2002, 2005) or indeed sampling stochasticity. For instance, a focus on oyster collection during the cooler seasons of the year in Context 5 may be related to a lack of resources as has been suggested elsewhere (Rowley-Conwy 1984, 2002), whilst environmental factors, including extreme tides or cooler waters, which may have been less inviting or indeed frozen, thus restricting access to the oyster beds, may have influenced the collection practices evidenced in Context 7 (Milner 2002; Milner 2005).

As yet, seasonality studies on Irish Mesolithic materials are vanishingly rare and tend to be based on other indicators than shellfish and/or incremental structures (**Figure 8**). In general, previous investigations into site occupation were based on the presence and/or absence of the recovered fauna whereby behavioural ecologies and habitat use were taken into account (e.g. Mitchell 1956; Liversage 1968). Perhaps the most detailed account of seasonality during the Irish Mesolithic is provided by Woodman et al. (1999) in their monograph on the site of Ferriter's Cove. Based on the presence of small

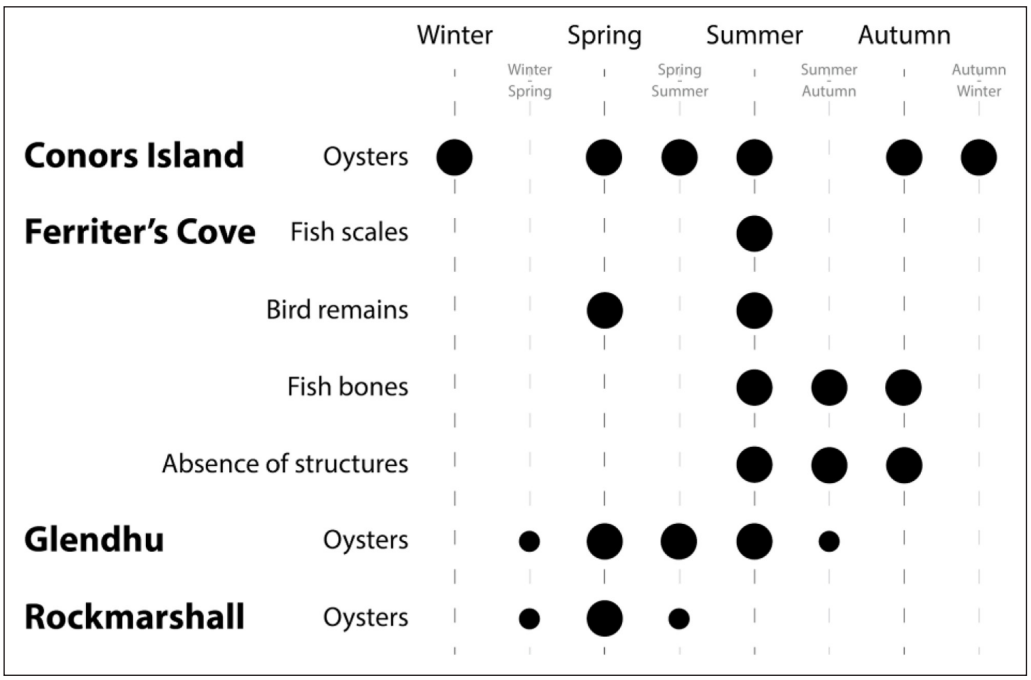

Figure 8: Seasonality indicators by site and by proxy for the Late Mesolithic in Ireland. Large circles indicate confident occupation, small circles indicate tentative occupation as a result of comparing seasonality data by Irving (1999), McCarthy (1999) and (Woodman 2001), which was grouped into four categories, with our data, which is grouped into eight categories.

gadids (codfishes), herring (*Clupea harengus*, Linnaeus, 1758), tope shark (*Galeorhinus galeus*, Linnaeus, 1758), salmon (salmons, trouts) and European eel (*Anguilla anguilla*, Linnaeus, 1758), McCarthy (1999) states that the site was occupied during the summer and autumn. Further to this, the presence of guillemot (*Uria aalge*, Pontoppidan, 1763) and a lack of structures suggested a summer presence, whilst the absence of migratory birds and seals (Phocidae) demonstrated that the site had not been occupied during the winter and spring. Moreover, the analysis of three ballan wrasse (*Labrus bergylta*, Ascanius, 1767) scales, which yielded identical growth patterns, and may be derived from the same individual, coupled with the presence of Sparidae (sea-breams, porgies), Labridae (wrasses), Mugilidae (grey mullets) and Triglidae (searobins, gurnards) scales demonstrated to Irving (1999) that capture and thus site occupation took place during the summer. Despite a degree of conjecture, these studies are in agreement with the results presented here, based on the elemental analysis. Indeed, only one study employing incremental growth-line analysis has been undertaken on Irish Mesolithic oysters, which demonstrated that Rockmarshall, Co. Louth, and Glendhu, Co. Down were occupied between the spring and summer (March–August) and spring (April–May) respectively (Woodman 2001). Despite the lack of detail concerning sample size, these data are likewise in agreement with the oyster collection practices at Conors Island.

5. Conclusion

This study demonstrates for the first time the potential of elemental mapping to analyse growth patterns in archaeological oyster shells through LIBS. Through extensive maps of Mg/Ca ratios, we determined the age and season of death with confidence for the majority of the analysed specimens (75% and 92%, respectively), and tentatively confirmed occupation of the Conors Island shell midden in almost all seasons of the year during the Late Mesolithic period. However, this dataset is preliminary and we expect the overall interpretation for the Sligo Bay area as well as the Irish Late Mesolithic to become more complex with an increase of seasonality data in the future.

We further demonstrate that rapid 2D mapping is essential in understanding the inter- and intra-specimen variability in Mg/Ca ratios, and that LIBS is able to provide the necessary amounts of specimens and data, in the form of elemental maps, at a low cost. This ability is beneficial for future seasonality studies that aim to include multiple sites or aim to increase individual site coverage. Low costs and fast analytical speeds are also beneficial for ecological studies, which aim to improve the overall robustness and representativity of the dataset and provide valuable information about shell size as well as biological age, which is necessary to differentiate between climatic and anthropogenic influence on shellfish productivity. For a more accurate interpretation of seasonality and biological age, future projects should also employ the use of additional geochemical proxies ($\delta^{18}O$), and modern shell specimens sourced directly from the Sligo Bay area.

Acknowledgements

This study was carried out as part of the Marie Skłodowska-Curie Individual Fellowship 'ACCELERATE' (Grant Agreement No. 703625). Chris Hunt thanks the Royal Irish Academy for an Excavation Grant and Finbar McCormick for leading the excavations of the Conors Island shell midden under licence no. 12E240. Initial survey and sampling was carried out under licence 0930174 and supported by funding from the Heritage Council of Ireland. Harry K. Robson should like to acknowledge the British Academy for funding. We further thank Demetrios Anglos and Panagiotis Siozos for their help in the lab, and Rhiannon Stevens for assistance with literature. Niklas Hausmann also acknowledges support by the project "HELLAS-CH" (MIS 5002735), implemented under the "Action for Strengthening Research and Innovation Infrastructures", funded by the Operational Programme "Competitiveness, Entrepreneurship and Innovation" (NSRF 2014-2020) and co-financed by Greece and the European Union (European Regional Development Fund). Lastly, we thank the two anonymous reviewers who's queries significantly improved the quality of this contribution.

Competing Interests

The authors have no competing interests to declare.

References

Andrus, CFT. 2011. Shell midden sclerochronology, *Quaternary science reviews*, 30(21–22): 2892–905. DOI: https://doi.org/10.1016/j.quascirev.2011.07.016

Andrus, CFT and **Crowe, DE.** 2000. Geochemical Analysis of *Crassostrea virginica* as a Method to Determine Season of Capture. *Journal of archaeological science*, 27(1): 33–42. DOI: https://doi.org/10.1006/jasc.1999.0417

Baggett, LP, Powers, SP, Brumbaugh, RD, Coen, LD, DeAngelis, BM, Greene, JK, Hancock, BT, Morlock, SM, Allen, BL, Breitburg, DL, Bushek, D, Grabowski, JH, Grizzle, RE, Grosholz, ED, La Peyre, MK, Luckenbach, MW, McGraw, KA, Piehler, MF, Westby, SR and **zu Ermgassen, PSE.** 2015. Guidelines for evaluating performance of oyster habitat restoration: Evaluating performance of oyster restoration. *Restoration Ecology*, 23(6): 737–45. DOI: https://doi.org/10.1111/rec.12262

Bailey, G and **Milner, N.** 2008. Molluscan archives from European prehistory. In *Early human impact on megamolluscs*, 1865: 111–34. Archaeopress Oxford.

Bayliss, A and **Woodman, PC.** 2009. A New Bayesian Chronology for Mesolithic Occupation at Mount Sandel, Northern Ireland. *Proceedings of the Prehistoric Society*, 75: 101–23. DOI: https://doi.org/10.1017/S0079497X00000311

Blitz, JH, Andrus, CFT and **Downs, LE.** 2014. Sclerochronological Measures of Seasonality at a Late Woodland Mound on the Mississippi Gulf Coast. *American antiquity*, 79(4): 697–711. DOI: https://doi.org/10.7183/0002-7316.79.4.697697

Bougeois, L, de Rafélis, M, Reichart, G-J, de Nooijer, LJ and **Dupont-Nivet, G.** 2016. Mg/Ca in fossil oyster

shells as palaeotemperature proxy, an example from the Palaeogene of Central Asia. *Palaeogeography, palaeoclimatology, palaeoecology*, 441: 611–26. DOI: https://doi.org/10.1016/j.palaeo.2015.09.052

Bougeois, L, de Rafélis, M, Reichart, G-J, de Nooijer, LJ, Nicollin, F and **Dupont-Nivet, G.** 2014. A high resolution study of trace elements and stable isotopes in oyster shells to estimate Central Asian Middle Eocene seasonality. *Chemical geology*, 363: 200–12. DOI: https://doi.org/10.1016/j.chemgeo.2013.10.037

Bronk Ramsey, C. 2017. OxCal Program, Version 4.3. *Oxford Radiocarbon Accelerator Unit: University of Oxford*. URL: https//c14.arch.ox.ac.uk/oxcal/OxCalhtml.

Burchell, M, Stopp, MP, Cannon, A, Hallmann, N and **Schöne, BR.** 2018. Determining seasonality of mussel collection from an early historic Inuit site, Labrador, Canada: Comparing thin-sections with high-resolution stable oxygen isotope analysis. *Journal of Archaeological Science: Reports*, 21: 1215–24. DOI: https://doi.org/10.1016/j.jasrep.2018.02.016

Cáceres, JO, Pelascini, F, Motto-Ros, V, Moncayo, S, Trichard, F, Panczer, G, Marín-Roldán, A, Cruz, JA, Coronado, I and **Martín-Chivelet, J.** 2017. Megapixel multi-elemental imaging by Laser-Induced Breakdown Spectroscopy, a technology with considerable potential for paleoclimate studies. *Scientific reports*, 7(1): 5080. DOI: https://doi.org/10.1038/s41598-017-05437-3

Cobo, A, García-Escárzaga, A, Gutiérrez-Zugasti, I, Setién, J, González-Morales, MR and **López-Higuera, JM.** 2017. Automated Measurement of Magnesium/Calcium Ratios in Gastropod Shells Using Laser-Induced Breakdown Spectroscopy for Paleoclimatic Applications. *Applied spectroscopy*, 71(4): 591–9. DOI: https://doi.org/10.1177/0003702816687570

Cobo, A, García-Escárzaga, A, Rodríguez-Cobo, L, Gutiérrez-Zugasti, I, González-Morales, MR and **López-Higuera, JM.** 2015. Automated Laser-induced Breakdown Spectroscopy setup for chemical mapping of archaeological shells. In *Advanced Photonics 2015*. JM3A.38, Novel Optical Materials and Applications, Optical Society of America. DOI: https://doi.org/10.1364/IPRSN.2015.JM3A.38

Dowd, M and **Carden, RF.** 2016. First evidence of a Late Upper Palaeolithic human presence in Ireland. *Quaternary science reviews*, 139: 158–63. DOI: https://doi.org/10.1016/j.quascirev.2016.02.029

Durham, SR, Gillikin, DP, Goodwin, DH and **Dietl, GP.** 2017. Rapid determination of oyster lifespans and growth rates using LA-ICP-MS line scans of shell Mg/Ca ratios. *Palaeogeography, palaeoclimatology, palaeoecology*, 485: 201–9. DOI: https://doi.org/10.1016/j.palaeo.2017.06.013

Edwards, R and **Brooks, A.** 2008. The island of Ireland: Drowning the myth of an Irish land-bridge? *The Irish naturalists' journal*, 29: 19–34.

Elliot, M, Welsh, K, Chilcott, C, McCulloch, M, Chappell, J and **Ayling, B.** 2009. Profiles of trace elements and stable isotopes derived from giant long-lived *Tridacna gigas* bivalves: Potential applications in paleoclimate studies. *Palaeogeography, palaeoclimatology, palaeoecology*, 280(1): 132–42. DOI: https://doi.org/10.1016/j.palaeo.2009.06.007

Epstein, S, Buchsbaum, R, Lowenstam, HA and **Urey, HC.** 1953. Revised Carbonate-water isotopic temperature scale. *Geological Society of America bulletin*, 64(11): 1315–26. DOI: https://doi.org/10.1130/0016-7606(1953)64[1315:RCITS]2.0.CO;2

Fan, C, Koeniger, P, Wang, H and **Frechen, M.** 2011. Ligamental increments of the mid-Holocene Pacific oyster *Crassostrea gigas* are reliable independent proxies for seasonality in the western Bohai Sea, China. *Palaeogeography, palaeoclimatology, palaeoecology*, 299(3): 437–48. DOI: https://doi.org/10.1016/j.palaeo.2010.11.022

Ferguson, JE, Henderson, GM, Fa, DA, Finlayson, JC and **Charnley, NR.** 2011. Increased seasonality in the Western Mediterranean during the last glacial from limpet shell geochemistry. *Earth and planetary science letters*, 308(3): 325–33. DOI: https://doi.org/10.1016/j.epsl.2011.05.054

Ford, HL, Schellenberg, SA, Becker, BJ, Deutschman, DL, Dyck, KA and **Koch, PL.** 2010. Evaluating the skeletal chemistry of *Mytilus californianus* as a temperature proxy: Effects of microenvironment and ontogeny. *Paleoceanography*, 25(1): PA1203. DOI: https://doi.org/10.1029/2008PA001677

Freitas, PS, Clarke, LJ, Kennedy, H and **Richardson, CA.** 2012. The potential of combined Mg/Ca and $\delta^{18}O$ measurements within the shell of the bivalve *Pecten maximus* to estimate seawater $\delta^{18}O$ composition. *Chemical geology*, 291: 286–93. DOI: https://doi.org/10.1016/j.chemgeo.2011.10.023

García-Escárzaga, A, Clarke, LJ, Gutiérrez-Zugasti, I, González-Morales, MR, Martinez, M, López-Higuera, J-M and **Cobo, A.** 2018. Mg/Ca profiles within archaeological mollusc (*Patella vulgata*) shells: Laser-Induced Breakdown Spectroscopy compared to Inductively Coupled Plasma-Optical Emission Spectrometry. *Spectrochimica acta. Part B: Atomic spectroscopy*, 148: 8–15. DOI: https://doi.org/10.1016/j.sab.2018.05.026

García-Escárzaga, A, Moncayo, S, Gutiérrez-Zugasti, I, González-Morales, MR, Martín-Chivelet, J and **Cáceres, JO.** 2015. Mg/Ca ratios measured by laser induced breakdown spectroscopy (LIBS): a new approach to decipher environmental conditions. *Journal of analytical atomic spectrometry*, 30(9): 1913–9. DOI: https://doi.org/10.1039/C5JA00168D

Gillikin, DP, Lorrain, A, Navez, J, Taylor, JW, André, L, Keppens, E, Baeyens, W and **Dehairs, F.** 2005. Strong biological controls on Sr/Ca ratios in aragonitic marine bivalve shells. *Geochemistry, Geophysics, Geosystems*, 6(5): Q05009. DOI: https://doi.org/10.1029/2004GC000874

Grabowski, JH and **Powers, SP.** 2004. Habitat complexity mitigates trophic transfer on oyster reefs. *Marine ecology progress series*, 277: 291–5. DOI: https://doi.org/10.3354/meps277291

Graniero, LE, Surge, D, Gillikin, DP, Briz i Godino, I and **Álvarez, M.** 2017. Assessing elemental ratios as a paleotemperature proxy in the calcite shells of patelloid limpets. *Palaeogeography, palaeoclimatology, palaeoecology*, 465: 376–85. DOI: https://doi.org/10.1016/j.palaeo.2016.10.021

Grant, J, Enright, CT and **Griswold, A.** 1990. Resuspension and growth of *Ostrea edulis*: A field experiment. *Marine biology*, 104(1): 51–9. DOI: https://doi.org/10.1007/BF01313157

Grossman, EL and **Ku, T-L.** 1986. Oxygen and carbon isotope fractionation in biogenic aragonite: Temperature effects. *Chemical Geology: Isotope Geoscience section*, 59: 59–74. DOI: https://doi.org/10.1016/0168-9622(86)90057-6

Gutiérrez-Zugasti, I. 2011. Coastal resource intensification across the Pleistocene–Holocene transition in Northern Spain: Evidence from shell size and age distributions of marine gastropods. *Quaternary international: the journal of the International Union for Quaternary Research*, 244(1): 54–66. DOI: https://doi.org/10.1016/j.quaint.2011.04.040

Gutiérrez-Zugasti, I, Andersen, SH, Araújo, AC, Dupont, C, Milner, N and **Monge-Soares, AM.** 2011. Shell midden research in Atlantic Europe: State of the art, research problems and perspectives for the future. *Quaternary International*, 239(1–2): 70–85. DOI: https://doi.org/10.1016/j.quaint.2011.02.031

Hallmann, N, Burchell, M, Schöne, BR, Irvine, GV and **Maxwell, D.** 2009. High-resolution sclerochronological analysis of the bivalve mollusk *Saxidomus gigantea* from Alaska and British Columbia: techniques for revealing environmental archives and archaeological seasonality. *Journal of archaeological science*, 36(10): 2353–64. DOI: https://doi.org/10.1016/j.jas.2009.06.018

Harding, JM, Mann, R, Southworth, MJ and **Wesson, JA.** 2010. Management of the Piankatank River, Virginia, in support of oyster (*Crassostrea virginica*, Gmelin 1791) fishery repletion. *Journal of shellfish research*, 29(4): 867–88. DOI: https://doi.org/10.2983/035.029.0421

Hausmann, N, Siozos, P, Lemonis, A, Colonese, AC, Robson, HK and **Anglos, D.** 2017. Elemental mapping of Mg/Ca intensity ratios in marine mollusc shells using laser-induced breakdown spectroscopy. *Journal of analytical atomic spectrometry*, 32(8): 1467–72. DOI: https://doi.org/10.1039/C7JA00131B

Hausmann, N and **Meredith-Williams, M.** 2017a. Seasonal Patterns of Coastal Exploitation on the Farasan Islands, Saudi Arabia. *The Journal of Island and Coastal Archaeology*, 12(3): 360–79. DOI: https://doi.org/10.1080/15564894.2016.1216478

Hausmann, N and **Meredith-Williams, M.** 2017b. Exploring Accumulation Rates of Shell Deposits Through Seasonality Data. *Journal of Archaeological Method and Theory*, 24(3): 776–95. DOI: https://doi.org/10.1007/s10816-016-9287-x

Hausmann, N, Prendergast, AL, Lemonis, A, Zech, J, Roberts, P, Siozos, P and **Anglos, D.** 2019a. Extensive elemental mapping unlocks Mg/Ca ratios as climate proxy in seasonal records of Mediterranean limpets. *Scientific reports*, 9(1): 3698. DOI: https://doi.org/10.1038/s41598-019-39959-9

Hausmann, N, Kokkinaki, O and **Leng, MJ.** 2019b. Red Sea Palaeoclimate: Stable Isotope and Element-Ratio Analysis of Marine Mollusc Shells. In *Geological Setting, Palaeoenvironment and Archaeology of the Red Sea*, Rasul, NMA and Stewart, ICF (eds.), 725–40. Cham: Springer International Publishing. DOI: https://doi.org/10.1007/978-3-319-99408-6_33

Hausmann, N, Prendergast, AL, Lemonis, A, Zech, J, Roberts, P, Siozos, P and **Anglos, D.** 2019c. LIBS Mapping of Mg/Ca ratios in marine mollusc shells. *protocols.io*. DOI: https://doi.org/10.17504/protocols.io.y7dfzi6

Hausmann, N, Robson, HK and **Hunt, C.** 2019d. Growth Incremental analysis of thin sections from marine molluscs. *protocols.io*. DOI: https://doi.org/10.17504/protocols.io.67chhiw

Irving, B. 1999. Fish Scales. In *Excavations at Ferriter's Cove 1983–95: first foragers, first farmers in the Dingle Peninsula*, Woodman, P, Anderson, E and Finlay, N (eds.), 92–3. Wordwell.

Kirby, MX, Soniat, TM and **Spero, HJ.** 1998. Stable isotope sclerochronology of Pleistocene and Recent oyster shells (*Crassostrea virginica*). *Palaios*, 13(6): 560–9. DOI: https://doi.org/10.2307/3515347

Kirby, MX and **Miller, HM.** 2005. Response of a benthic suspension feeder (*Crassostrea virginica*) to three centuries of anthropogenic eutrophication in Chesapeake Bay. *Estuarine, coastal and shelf science*, 62(4): 679–89. DOI: https://doi.org/10.1016/j.ecss.2004.10.004

Kraeuter, JN, Ford, S and **Cummings, M.** 2007. Oyster Growth Analysis: A comparison of methods. *Journal of shellfish research*, 26(2): 479–91. DOI: https://doi.org/10.2983/0730-8000(2007)26[479:OGAACO]2.0.CO;2

Kusnerik, KM, Lockwood, R and **Grant, AN.** 2018. Using the Fossil Record to Establish a Baseline and Recommendations for Oyster Mitigation in the Mid-Atlantic U.S. In *Marine Conservation Paleobiology*, Tyler, CL and Schneider, CL (eds.), 75–103. Cham: Springer International Publishing. DOI: https://doi.org/10.1007/978-3-319-73795-9_5

Levinton, J, Doall, M and **Allam, B.** 2013. Growth and mortality patterns of the eastern oyster *Crassostrea virginica* in impacted waters in coastal waters in New York, USA. *Journal of shellfish research*, 32(2): 417–27. DOI: https://doi.org/10.2983/035.032.0222

Little, A, van Gijn, A, Collins, T, Cooney, G, Elliott, B, Gilhooly, B, Charlton, S and **Warren, G.** 2017. Stone Dead: Uncovering Early Mesolithic Mortuary

Rites, Hermitage, Ireland. *Cambridge Archaeological Journal*, 27(2): 223–43. DOI: https://doi.org/10.1017/S0959774316000536

Liversage, GD. 1968. Excavations at Dalkey Island, Co. Dublin, 1956–1959. Royal Irish Academy.

Lulewicz, IH, Thompson, VD, Pluckhahn, TJ, Andrus, CFT and **Das, O.** 2018. Exploring Oyster (*Crassostrea virginica*) Habitat Collection via Oxygen Isotope Geochemistry and its Implications for Ritual and Mound Construction at Crystal River and Roberts Island, Florida. *The Journal of Island and Coastal Archaeology*, 13(3): 388–404. DOI: https://doi.org/10.1080/15564894.2017.1363096

Lutz, RA and **Rhoads, DC.** 1977. Anaerobiosis and a theory of growth line formation. *Science*, 198(4323): 1222–7. DOI: https://doi.org/10.1126/science.198.4323.1222

Lutz, RA and **Rhoads, DC.** 1980. Growth Patterns within the Molluscan Shell. In *Skeletal Growth of Aquatic Organisms*, Rhoads, DC and Lutz, RA (eds.), 203–54. Topics in Geobiology, Springer US, Boston, MA. DOI: https://doi.org/10.1007/978-1-4899-4995-0_7

Mannino, MA and **Thomas, KD.** 2001. Intensive Mesolithic Exploitation of Coastal Resources? Evidence from a Shell Deposit on the Isle of Portland (Southern England) for the Impact of Human Foraging on Populations of Intertidal Rocky Shore Molluscs. *Journal of archaeological science*, 28(10): 1101–14. DOI: https://doi.org/10.1006/jasc.2001.0658

Mannino, MA and **Thomas, KD.** 2002. Depletion of a resource? The impact of prehistoric human foraging on intertidal mollusc communities and its significance for human settlement, mobility and dispersal. *World archaeology*, 33(3): 452–74. DOI: https://doi.org/10.1080/00438240120107477

Mannino, MA, Spiro, BF and **Thomas, KD.** 2003. Sampling shells for seasonality: oxygen isotope analysis on shell carbonates of the inter-tidal gastropod *Monodonta lineata* (da Costa) from populations across its modern range and from a Mesolithic site in southern Britain. *Journal of archaeological science*, 30(6): 667–79. DOI: https://doi.org/10.1016/S0305-4403(02)00238-8

McCarthy, A. 1999. Faunal remains. In *Excavations at Ferriter's Cove 1983–95: first foragers, first farmers in the Dingle Peninsula*, Woodman, P, Anderson, E and Finlay, N (eds.), 85–92. Wordwell.

Milner, N. 2001. At the Cutting Edge: Using Thin Sectioning to Determine Season of Death of the European Oyster, *Ostrea edulis*. *Journal of archaeological science*, 28(8): 861–73. DOI: https://doi.org/10.1006/jasc.2000.0618

Milner, N. 2002. *Incremental Growth of the European Oyster, Ostrea edulis: seasonality information from Danish kitchenmiddens*, Vol. 1057. British Archaeological Reports Limited.

Milner, N. 2005. Can seasonality studies be used to identify sedentism in the past. Bailey, D, Whittle, A and Cummings, V (eds.), 32–7.

Milner, N and **Woodman, PC.** 2007. Deconstructing the myths of Irish shell middens. *Shell Middens in Atlantic Europe*, 101.

Milner, N and **Laurie, E.** 2009. Coastal Perspectives on the Mesolithic—Neolithic Transition. *Mesolithic Horizons*, 134–9.

Mitchell, GF. 1956. An Early Kitchen-Midden at Sutton, Co. Dublin (Studies in Irish Quaternary Deposits: No. 12). *Journal of the Royal Society of Antiquaries of Ireland*, 86(1): 1–26.

Mouchi, V, de Rafélis, M, Lartaud, F, Fialin, M and **Verrecchia, E.** 2013. Chemical labelling of oyster shells used for time-calibrated high-resolution Mg/Ca ratios: A tool for estimation of past seasonal temperature variations. *Palaeogeography, palaeoclimatology, palaeoecology*, 373: 66–74. DOI: https://doi.org/10.1016/j.palaeo.2012.05.023

Mouchi, V, Briard, J, Gaillot, S, Argant, T, Forest, V and **Emmanuel, L.** 2018. Reconstructing environments of collection sites from archaeological bivalve shells: Case study from oysters (Lyon, France). *Journal of Archaeological Science: Reports*, 21: 1225–35. DOI: https://doi.org/10.1016/j.jasrep.2017.10.025

Murray, E. 2009. A Late Mesolithic Shell Midden at Tullybeg, Co. Galway. *Journal of the Galway Archaeological and Historical Society*, 61: 1–3.

Orton, JH. 1928. On Rhythmic Periods in Shell-growth in 0. edulis with a Note on Fattening. *Journal of the Marine Biological Association of the United Kingdom*, 15(2): 365–427. DOI: https://doi.org/10.1017/S0025315400009498

Poulain, C, Gillikin, DP, Thébault, J, Munaron, J-M, Bohn, M, Robert, R, Paulet, Y-M and **Lorrain, A.** 2015. An evaluation of Mg/Ca, Sr/Ca, and Ba/Ca ratios as environmental proxies in aragonite bivalve shells. *Chemical geology*, 396: 42–50. DOI: https://doi.org/10.1016/j.chemgeo.2014.12.019

Powell, EN, Ashton-Alcox, KA, Kraeuter, JN, Ford, SE and **Bushek, D.** 2008. Long-term Trends in Oyster Population Dynamics in Delaware Bay: Regime Shifts and Response to Disease. *Journal of shellfish research*, 27(4): 729–55. DOI: https://doi.org/10.2983/0730-8000(2008)27[729:LTIOPD]2.0.CO;2

Prendergast, AL and **Stevens, RE.** 2014. Molluscs (Isotopes): Analyses in Environmental Archaeology. In *Encyclopedia of Global Archaeology*, Smith, C (ed.), 5010–9. New York: Springer. DOI: https://doi.org/10.1007/978-1-4419-0465-2_2162

Reimer, PJ, Bard, E, Bayliss, A, Warren Beck, J, Blackwell, PG, Ramsey, CB, Buck, CE, Cheng, H, Lawrence Edwards, R, Friedrich, M, Grootes, PM, Guilderson, TP, Haflidason, H, Hajdas, I, Hatté, C, Heaton, TJ, Hoffmann, DL, Hogg, AG, Hughen, KA, Felix Kaiser, K, Kromer, B, Manning, SW, Niu, M, Reimer, RW, Richards, DA, Marian Scott, E, Southon, JR, Staff, RA, Turney, CSM and **van der Plicht, J.** 2013. IntCal13 and Marine13 Radiocarbon Age Calibration Curves 0–50,000 Years cal BP. *Radiocarbon*,

55(4): 1869–87. DOI: https://doi.org/10.2458/azu_js_rc.55.16947

Rick, TC and **Lockwood, R.** 2013. Integrating paleobiology, archeology, and history to inform biological conservation. *Conservation biology: the journal of the Society for Conservation Biology*, 27(1): 45–54. DOI: https://doi.org/10.1111/j.1523-1739.2012.01920.x

Rick, TC, Reeder-Myers, LA, Hofman, CA, Breitburg, D, Lockwood, R, Henkes, G, Kellogg, L, Lowery, D, Luckenbach, MW, Mann, R, Ogburn, MB, Southworth, M, Wah, J, Wesson, J and **Hines, AH.** 2016. Millennial-scale sustainability of the Chesapeake Bay Native American oyster fishery. *Proceedings of the National Academy of Sciences of the United States of America*, 113(23): 6568–73. DOI: https://doi.org/10.1073/pnas.1600019113

Rick, TC, Reeder-Myers, LA, Carr, MJ and **Hines, AH.** 2017. 3000 Years of Human Subsistence and Estuarine Resource Exploitation on the Rhode River Estuary, Chesapeake Bay, Maryland. *Journal of the North Atlantic*, 10(10): 113–25. DOI: https://doi.org/10.3721/037.002.sp1011

Rifai, K, Doucet, F, Özcan, L and **Vidal, F.** 2018. LIBS core imaging at kHz speed: Paving the way for real-time geochemical applications. *Spectrochimica acta. Part B: Atomic spectroscopy*, 150: 43–8. DOI: https://doi.org/10.1016/j.sab.2018.10.007

Robson, H. 2015. Evaluating the change of consumption and culinary practices at the transition to agriculture: a multi-disciplinary approach from a Danish kitchen midden, Phd, University of York.

Rowley-Conwy, P. 1984. The laziness of the short-distance hunter: The origins of agriculture in western Denmark. *Journal of Anthropological Archaeology*, 3(4): 300–24. DOI: https://doi.org/10.1016/0278-4165(84)90005-9

Rowley-Conwy, P. 2002. The Laziness of the Short-Distance Hunter: the origins of agriculture in western Denmark. In *The Neolithisation of Denmark*, Fischer, A and Kristiansen, K (eds.), 273–87.

Savarese, M, Walker, KJ, Stingu, S, Marquardt, WH and **Thompson, V.** 2016. The effects of shellfish harvesting by aboriginal inhabitants of Southwest Florida (USA) on productivity of the eastern oyster: Implications for estuarine management and restoration. *Anthropocene*, 16: 28–41. DOI: https://doi.org/10.1016/j.ancene.2016.10.002

Schöne, BR, Zhang, Z, Jacob, D, Gillikin, DP, Tütken, T, Garbe-Schönberg, D and **Soldati, A.** 2010. Effect of organic matrices on the determination of the trace element chemistry (Mg, Sr, Mg/Ca, Sr/Ca) of aragonitic bivalve shells (*Arctica islandica*)—Comparison of ICP-OES and LA-ICP-MS data. *Geochemical journal*, 44(1): 23–37. DOI: https://doi.org/10.2343/geochemj.1.0045

Schöne, BR, Zhang, Z, Radermacher, P, Thébault, J, Jacob, DE, Nunn, EV and **Maurer, A-F.** 2011. Sr/Ca and Mg/Ca ratios of ontogenetically old, long-lived bivalve shells (*Arctica islandica*) and their function as paleotemperature proxies. *Palaeogeography, palaeoclimatology, palaeoecology*, 302(1): 52–64. DOI: https://doi.org/10.1016/j.palaeo.2010.03.016

Schöne, BR, Radermacher, P, Zhang, Z and **Jacob, DE.** 2013. Crystal fabrics and element impurities (Sr/Ca, Mg/Ca, and Ba/Ca) in shells of *Arctica islandica*—implications for paleoclimate reconstructions. *Palaeogeography, palaeoclimatology, palaeoecology*, 373: 50–9. DOI: https://doi.org/10.1016/j.palaeo.2011.05.013

Surge, D, Lohmann, KC and **Dettman, DL.** 2001. Controls on isotopic chemistry of the American oyster, *Crassostrea virginica*: implications for growth patterns. *Palaeogeography, palaeoclimatology, palaeoecology*, 172(3): 283–96. DOI: https://doi.org/10.1016/S0031-0182(01)00303-0

Thompson, VD and **Andrus, CFT.** 2011. Evaluating Mobility, Monumentality, and Feasting at the Sapelo Island Shell Ring Complex. *American antiquity*, 76(2): 315–43. DOI: https://doi.org/10.7183/0002-7316.76.2.315

Twaddle, RW, Ulm, S, Hinton, J, Wurster, CM and **Bird, MI.** 2016. Sclerochronological analysis of archaeological mollusc assemblages: methods, applications and future prospects. *Archaeological and anthropological sciences*, 8(2): 359–79. DOI: https://doi.org/10.1007/s12520-015-0228-5

Tynan, S, Opdyke, BN, Walczak, M, Eggins, S and **Dutton, A.** 2017. Assessment of Mg/Ca in *Saccostrea glomerata* (the Sydney rock oyster) shell as a potential temperature record. *Palaeogeography, palaeoclimatology, palaeoecology*, 484: 79–88. DOI: https://doi.org/10.1016/j.palaeo.2016.08.009

Waddell, J. 2010. *The prehistoric archaeology of Ireland*. Dubline: Wordwell.

Walne, PR. 1958. Growth of oysters (*Ostrea edulis* L.). *Journal of the Marine Biological Association of the United Kingdom*, 37(3): 591–602. DOI: https://doi.org/10.1017/S0025315400005634

Wanamaker, AD, Jr., Kreutz, KJ, Wilson, T, Borns, HW, Jr., Introne, DS and **Feindel, S.** 2008. Experimentally determined Mg/Ca and Sr/Ca ratios in juvenile bivalve calcite for *Mytilus edulis*: implications for paleotemperature reconstructions. *Geo-Marine Letters*, 28(5): 359–68. DOI: https://doi.org/10.1007/s00367-008-0112-8

West, CF, Burchell, M and **Andrus, CFT.** 2018. Molluscs and Paleoenvironmental Reconstruction in Island and Coastal Settings: Variability, Seasonality, and Sampling. In *Zooarchaeology in Practice: Case Studies in Methodology and Interpretation in Archaeofaunal Analysis*, Giovas, CM and LeFebvre, MJ (eds.), 191–208. Cham: Springer International Publishing. DOI: https://doi.org/10.1007/978-3-319-64763-0_10

Woodman, PC. 1985. *Excavations at Mount Sandel, 1973–77, County Londonderry*. HM Stationery Office.

Woodman, PC, Anderson, E and **Finlay, N.** 1999. *Excavations at Ferriter's Cove, 1983–95: Last Foragers, First Farmers in the Dingle Peninsula*. Dublin, Ireland: Wordwell.

Woodman, PC. 2001. Mesolithic middens: from famine to feasting. *Archaeology Ireland*, 15(3): 32–5.

Woodman, PC and **Milner, N.** 2013. "From restaurant to take-away": placing Sligo shell middens in context. In *Dedicated to Sligo: Thirty-Four Essays on Sligo's Past*, Timoney, MA (ed.), 37–40. Ballmote.

Woodman, PC. 2015. *Ireland's First Settlers: time and the Mesolithic*. Oxford: Oxbow.

Zimmt, JB, Lockwood, R, Andrus, CFT and **Herbert, GS.** 2019. Sclerochronological basis for growth band counting: A reliable technique for life-span determination of *Crassostrea virginica* from the mid-Atlantic United States. *Palaeogeography, palaeoclimatology, palaeoecology*, 516: 54–63. DOI: https://doi.org/10.1016/j.palaeo.2018.11.029

How to cite this article: Hausmann, N, Robson, HK and Hunt, C. 2019. Annual Growth Patterns and Interspecimen Variability in Mg/Ca Records of Archaeological *Ostrea edulis* (European Oyster) from the Late Mesolithic Site of Conors Island. *Open Quaternary*, 5: 9, pp. 1–18. DOI: https://doi.org/10.5334/oq.59

Submitted: 14 March 2019 **Accepted:** 13 September 2019 **Published:** 30 September 2019

]u[*Open Quaternary* is a peer-reviewed open access journal published by Ubiquity Press. OPEN ACCESS